Towards an Investigation of the Effects of Dynamic Topography on Vertical Land Motions Along the North American Atlantic Coast

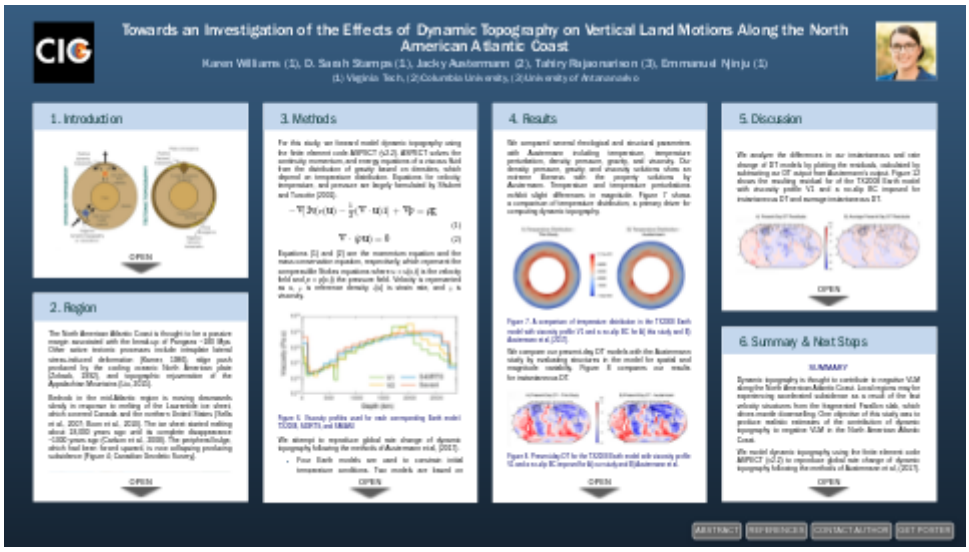

Karen Williams (1), D. Sarah Stamps (1), Jacky Austermann (2), Tahiry Rajaonarison (3), Emmanuel Njinju (1)

(1) Virginia Tech, (2) Columbia University, (3) University of Antananarivo

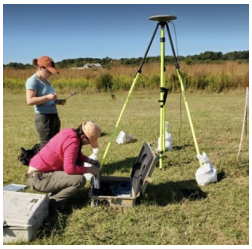




PRESENTED AT:

1. INTRODUCTION

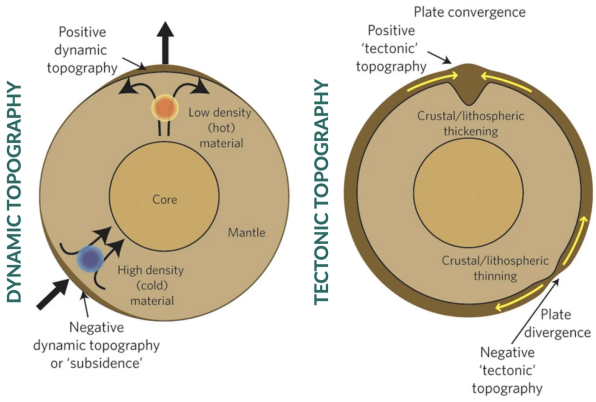

Figure 1. Left: Sketch illustrating the impact of mantle flow on dynamic surface topography. The red and blue circles represent low (hot) and high (cold) density anomalies. The black arrows represent induced mantle flow and resulting dynamic surface topography. Right: Isostatically conpensated tectonic topography driven by thinning or thickening of the lithosphere (including the crust) in response to tectonic plate motions represented by the yellow arrows (Braun, 2010).

Dynamic topography (DT), defined as the deflection of the Earth's surface due to the convecting mantle, causes changes in vertical land motions (VLM; Molnar et al. 2015). This definition of dynamic topography does not include crustal isostastically induced tectonic topography. Figure 1 illustrates how surface deformation are generated by dynamic topography versus tectonic topography.

Analyzing the influence of mantle convection on vertical motion measurements is challenging due to uncertainties in Earth's structure, including thickness and rheology, as well as temperature and density distributions and anomalies (Rowley et al., 2013; Gurnis and Yang, 2016). In turn, present-day global dynamic topography models show wide variabilty spatially and in magnitude (Fig 2; Rubey et al. 2017).

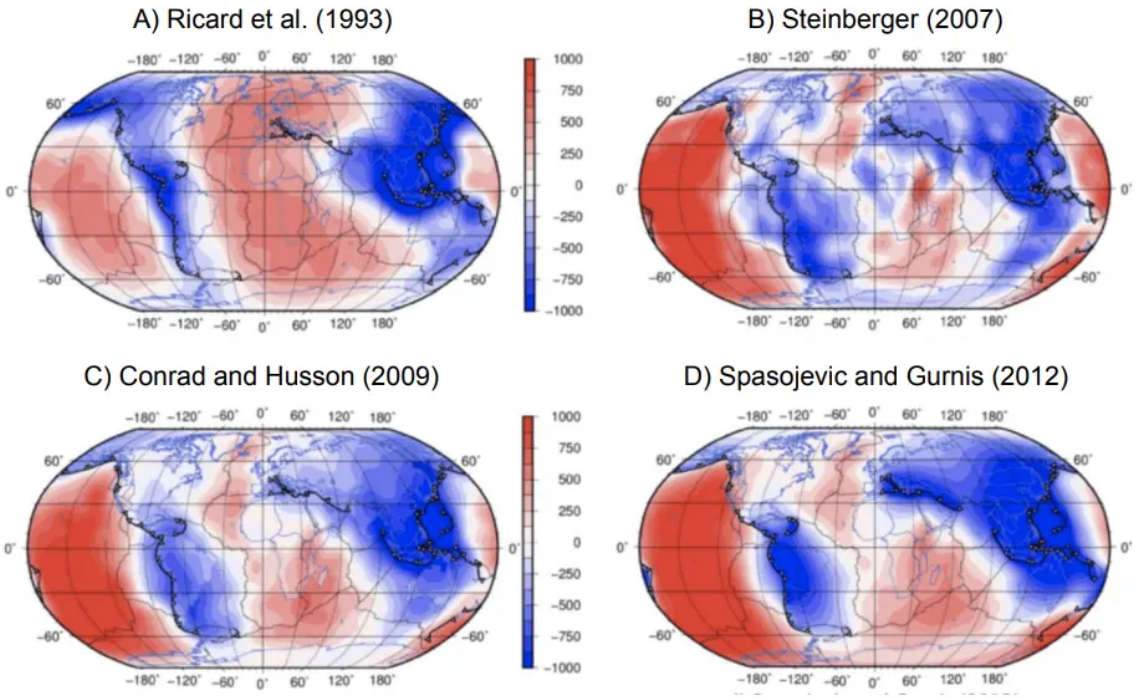

Figure 2. Comparison of global, present-day dynamic topography models from A) Ricard et al, (1993), B) Steinberger, (2007), C) Conrad and Husson, (2009), D) Spasojevic and Gurnis, (2012)

Dynamic topography is thought to contribute to VLM along the North American Atlantic Coast. Prior studies indicate negative VLM (i.e. subsidence) in the mid-Atlantic region (Figure 3; Hammond et al, 2021). However, these studies show discrepencies in spatial resolution and rate of change.

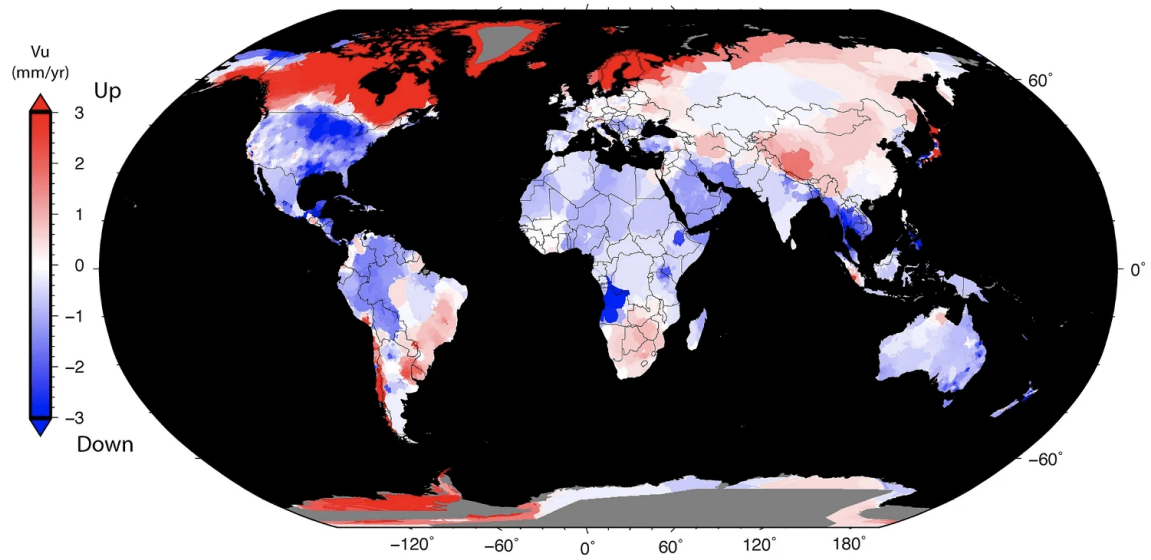

Figure 3. GPS Imaging of vertical land motions derived from continuously operating GPS stations processed by the Nevada Geodetic Laboratory.

Subsidence is particularly important to constrain because of its implications for coastal hazards including relative sea-level rise and nuisance flooding. Additionally, the North American Atlantic Coast has a history of accelerated local subsidence from groundwater extraction. Improved estimates of rate change of dynamic topography will allow us to better isolate the contribution of DT to VLM along the North American Atlantic Coast from external processes including glacial isostatic adjustment and, therefore, groundwater extraction, which can help inform ecological reserachers for aquifer management decisions. We hypothesize that the North American Atlantic Coast is experiencing regional land subsidence, accelerated by a slight contribution (<1 mm/yr) from negative dynamic topography.

2. REGION

The North American Atlantic Coast is thought to be a passive margin associated with the break-up of Pangaea ~180 Mya. Other active tectonic processes include intraplate lateral stress-induced deformation (Karner, 1986), ridge push produced by the cooling oceanic North American plate (Zoback, 1992), and topographic rejuvenation of the Appalachian Mountains (Liu, 2015).

Bedrock in the mid-Atlantic region is moving downwards slowly in response to melting of the Laurentide ice sheet, which covered Canada and the northern United States (Sella et al., 2007; Boon et al., 2010). The ice sheet started melting about 18,000 years ago until its complete disappearance ~1000 years ago (Carlson et al., 2008). The peripheral bulge, which had been forced upward, is now collapsing producing subsidence (Figure 4; Canadian Geodetic Survey).

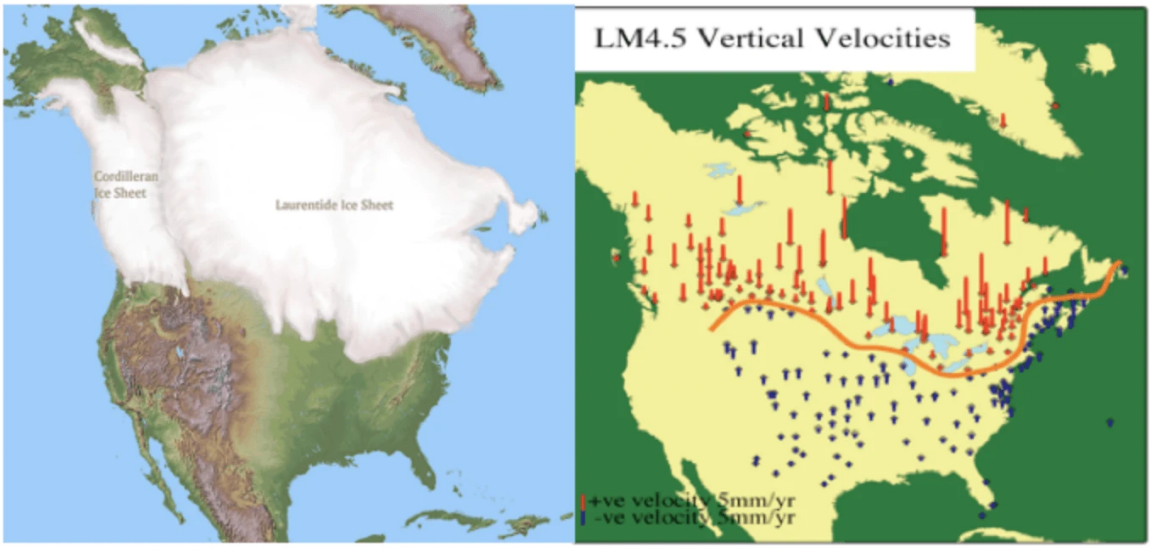

Figure 4. Left: Extent of the Laurentide ice sheet at the Last Glacial Maximum. Right: GIA predictions for North America. Red vectors indicate uplift, while blue vectors indicate subsidence. The orange line depicts where deformation changes from positive to negative.

Additionally, the ~100 million year old fragmented Farallon slab lies beneath the North American Atlantic Coast, which has been imaged with seismic tomography (i.e. Schmid et al., 2002; Figure 6b). Global tomography models of the mantle beneath the North American Atlantic Coast indicate seismically fast velocities beneath the region between 1300-1750 km depths (i.e. Lu et al., 2019). The fast velocity structures suggest cold and/or compositionally dense structures in the deep mantle, inducing mantle downwelling, which is hypothesized to promote negative dynamic topography (Lithgow-Bertelloni and Gurnis, 1997; Spasojević et al., 2008).

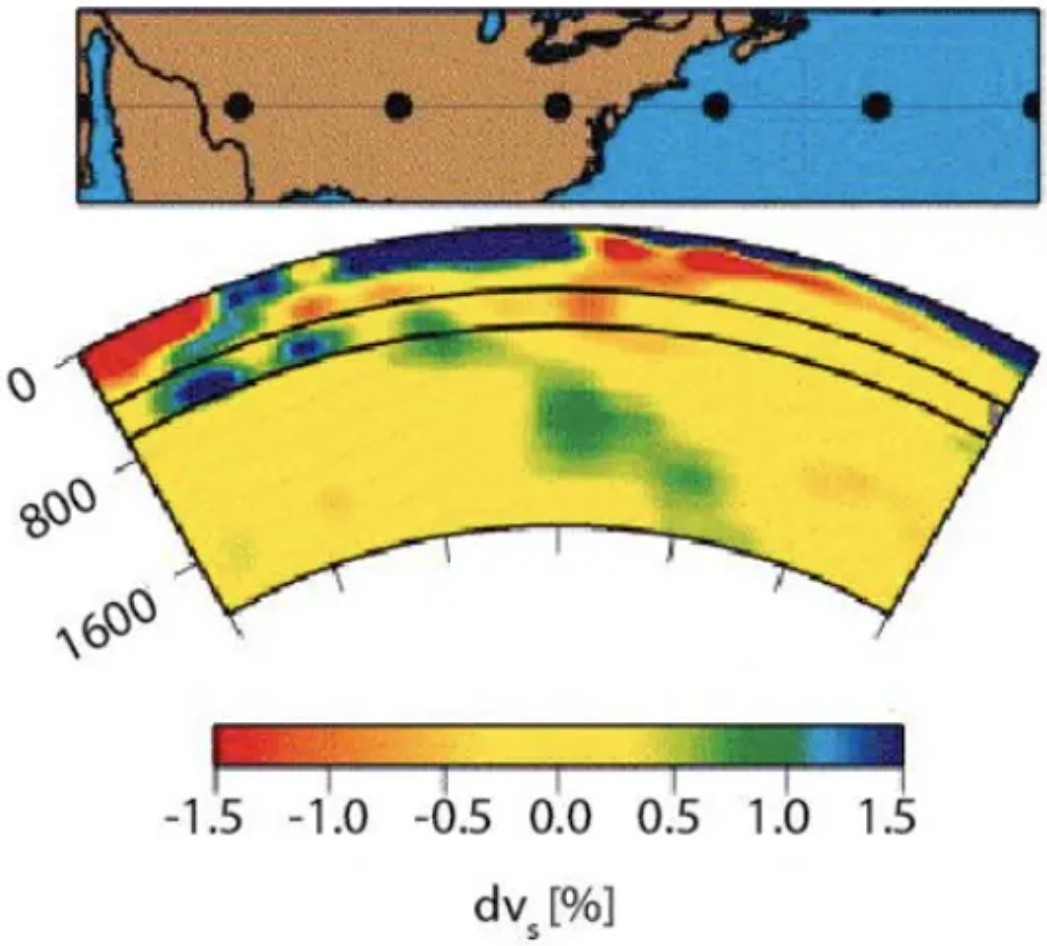

Figure 5. Shear-wave tomography derived image of the Farallon slab

3. METHODS

For this study, we forward model dynamic topography using the finite element code ASPECT (v2.2). ASPECT solves the continuity, momentum, and energy equations of a viscous fluid from the distribution of gravity based on densities, which depend on temperature distribution. Equations for velocity, temperature, and pressure are largely formulated by Shubert and Turcotte (2001).

$$-\nabla[2\eta(\epsilon(\mathbf{u}) - \tfrac{1}{3}(\nabla \cdot \mathbf{u})1] + \nabla p = \rho \mathbf{g} \quad (1)$$

$$\nabla \cdot (\rho \mathbf{u}) = 0 \quad (2)$$

Equations (1) and (2) are the momentum equation and the mass conservation equation, respectively, which represent the compressible Stokes equations where u = u(x,t) is the velocity field and p = p(x,t) the pressure field. Velocity is represented as u, ρ is reference density, ϵ(u) is strain rate, and η is viscosity.

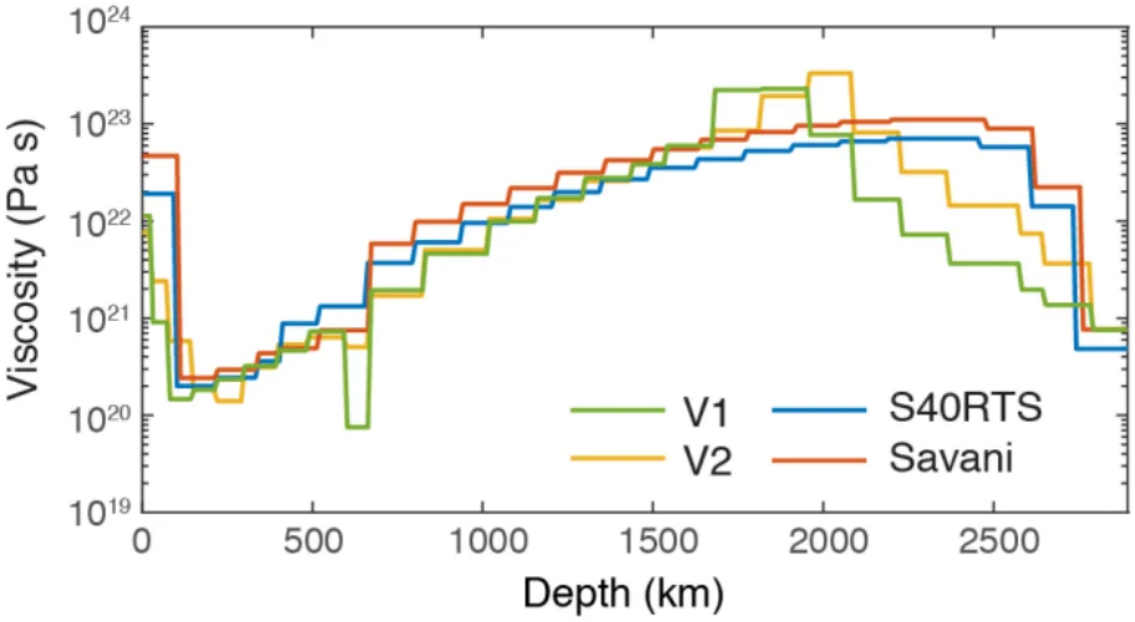

Figure 6. Viscosity profiles used for each corresponding Earth model: TX2008, S40RTS, and SAVANI

We attempt to reproduce global rate change of dynamic topography following the methods of Austermann et al, (2017).

- Four Earth models are used to constrain initial temperature conditions. Two models are based on density model TX2008, with corresponding radial visocity profiles, V1 and V2 (Figure 6, Austermann et al, 2017).
- The two additional Earth models are based on shear-wave tomorgraphy models, S40RTS (Ritsema et al, 2011) and SAVANI (Auer et al, 2014).
- Depth and buoyancy of the continental lithosphere is parameterized by Steinberger (2016) with a specfic depth-dependent visocity profile set for the two tomography models (Figure 6).
- We impose a radial varying gravity profile from Glisovic and Forte, (2014).
- Each Earth model is tested with three different boundary conditions (BC): no-slip, free slip, and prescribed plate motions velocites from GPlates.

Several model properties and instantaneous dynamic topgraphy are evaluated for comparison with solutions by Austermann.

The following equations are used to compute dynamic topography.

$$\sigma_{rr} = \hat{g}^T(2\eta\varepsilon(\mathbf{u}) - \tfrac{1}{3}(\text{div } \mathbf{u})I)\hat{g} - p_d \quad (3)$$

$$\hat{g} = \mathbf{g}/\|\mathbf{g}\| \quad p_d = p - p_a$$

$$h = \frac{\sigma_{rr}}{(\mathbf{g}\cdot\mathbf{n})\rho} \tag{4}$$

Equation (3) is computes stress tensors, where $\hat{g}$ is the direction of gravity and ρ is density.

We use MATLAB to calculate rate changes of dynamic topography between ~2 Mya and ~1 Mya in model time. We obtain average DT and average rate change of DT by averaging the instantaneous and rate change of DT in each grid space (increments of 0.5 longitudes and latitudes) between 6 selected models.

In this study, we also aim to test the consistent boundary flux (CBF) algorithm for determining radial stresses at the boundaries, which was implemented into ASPECT in 2019 and significantly improves the accuracy of the geoid and dynamic topography calculation. By replicating the model setups and methodoloigy by Austermann, we can constrain the influence of the CBF algorithm.

Our results focus on runs completed with the TX2008 Earth model. Modifications made to ASPECT following Austermann et al, (2017) have created challenges in replicating model setups using S40RTS and SAVANI and isolating the influence of the CBF algorithm on DT.

4. RESULTS

We compared several rheological and structural parameters with Austermann including temperature, temperature perturbation, density, pressure, gravity, and viscosity. Our density, pressure, gravity, and viscosity solutions show an extreme likeness with the property solutions by Austermann. Temperature and temperature perturbations exhibit slight differences in magnitude. Figure 7 shows a comparison of temperature distribution, a primary driver for computing dynamic topography.

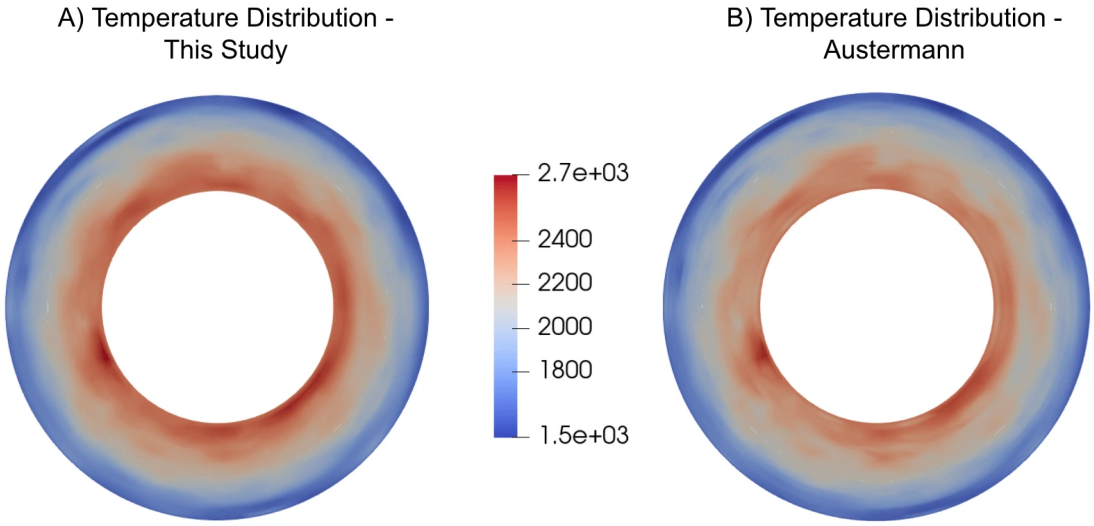

Figure 7. A comparison of temperature distribution in the TX2008 Earth model with viscosity profile V1 and a no-slip BC for A) this study and B) Austermann et al, (2017).

We compare our present-day DT models with the Austermann study by evaluating structures in the model for spatial and magnitude variabilty. Figure 8 compares our results for instantaneous DT.

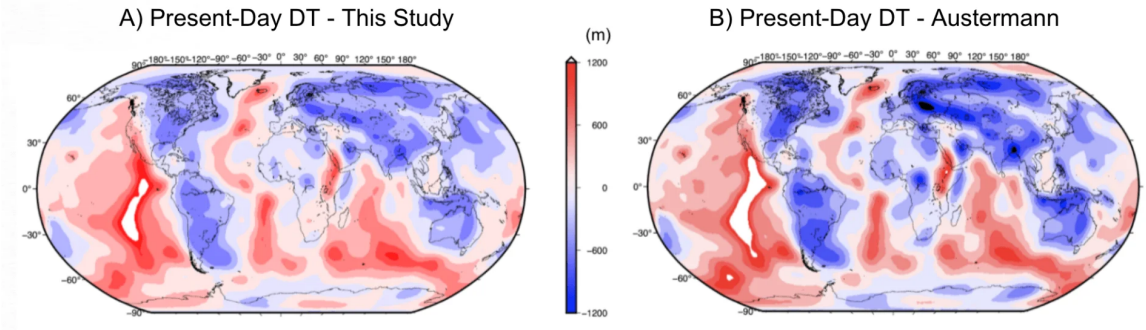

Figure 8. Present-day DT for the TX2008 Earth model with viscosity profile V1 and a no-slip BC imposed for A) our study and B) Austermann et al.

We tested a total of 6 model setups with the TX2008 Earth model, which vary by radial viscosity profile and boundary conditions applied. Table 1 lists the range for instantaneous DT for our 6 models. Figure 9 compares the average instantaneous DT for all 6 TX2008 Earth models setups.

TX2008 Earth Model Viscosity Profile / Boundary Condition	Present-Day DT Min / Max (m) **This Study**	Present-Day DT Min / Max (m) **Austermann**	Present-Day DT | Average Min/Max Difference |
V1 / No-Slip	-914 / 1521	-1355 / 1859	51.5
V1 / Free Slip	-1343 / 1842	-1660 / 2192	16.5
V1 / Gplates	-2903 / 5999	-3577 / 6089	292
V2 / No-Slip	-943 / 1438	-1423 / 1782	68
V2 / Free Slip	-1340 / 1792	-1400 / 1765	43.5
V2 / Gplates	-2341 / 4725	-2093 / 3551	463

Table 1. The left column lists the viscosity profile and the boundary conditions applied to each model setup. The middle column and right column provide minimum and maximum values of instantaneous DT for our study and Austermann et al, (2017), respectively.Figure 9. Average present-day DT calculated from the 6 TX2008 Earth models for A) our study and B) Austermann et al, (2017).

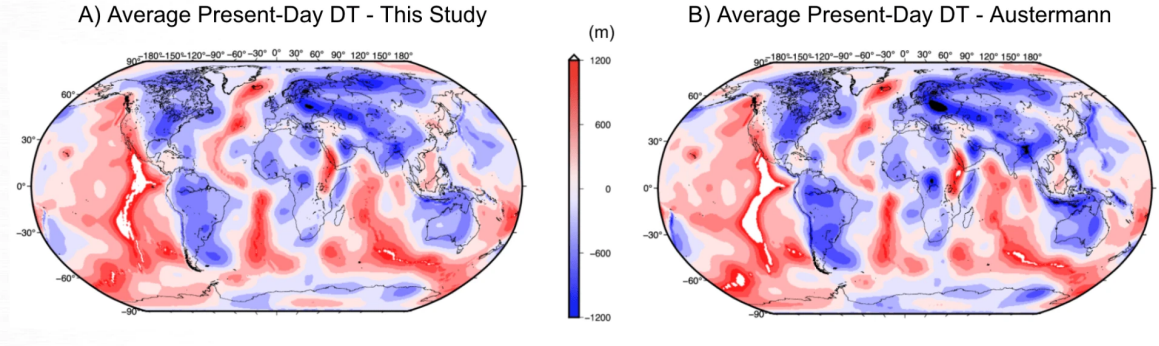

Figure 9. Average present-day DT calculated from the 6 TX2008 Earth models for A) our study and B) Austermann et al, (2017).

Rate change of DT is computed between ~2 Mya and ~1 Mya. Figure 10 compares rate change of dynamic topography for the same model setup used to calcluate instantaneous DT in Figure 8.

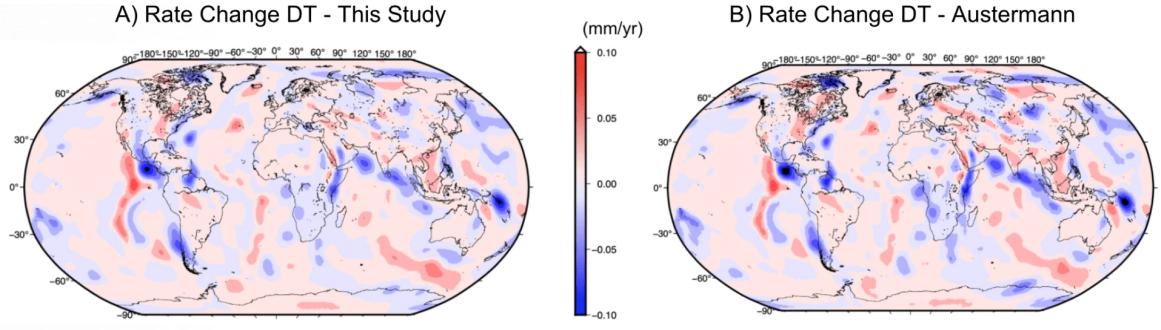

Figure 10. Rate change of DT for TX2008 Earth model with viscosity profile V1 and a no-slip BC imposed for A) our study and B) Austermann et al, (2017).

Table 2 lists the minimum and maximum values for rate change of DT for each TX2008 Earth model setup.

TX2008 Earth Model Viscosity Profile / Boundary Condition	DT Rate Change Min / Max (mm/yr) **This Study**	DT Rate Change Min / Max (mm/yr) **Austermann**	Rate Change DT |Average Min/Max Difference (mm/yr)|
V1 / No-Slip	-0.106 / 0.077	-0.120 / 0.080	0.0055
V1 / Free Slip	-0.167 / 0.159	-0.249 / 0.263	0.011
V1 / Gplates	-0.231 / 0.262	-0.162 / 0.304	0.0555
V2 / No-Slip	-0.072 / 0.051	-0.050 / 0.031	0.001
V2 / Free Slip	-0.114 / 0.120	-0.169 / 0.212	0.0185
V2 / Gplates	-0.212 / 0.280	-0.121 / 0.241	0.026

Table 2. Minimum and maximum values for rate change of DT for all TX2008 Earth model setups

Our final rate of change of DT solution was calculated by averaging rate change of DT for the 6 TX2008 Earth model setups. Figure 11 shows our final rate change of DT solution.

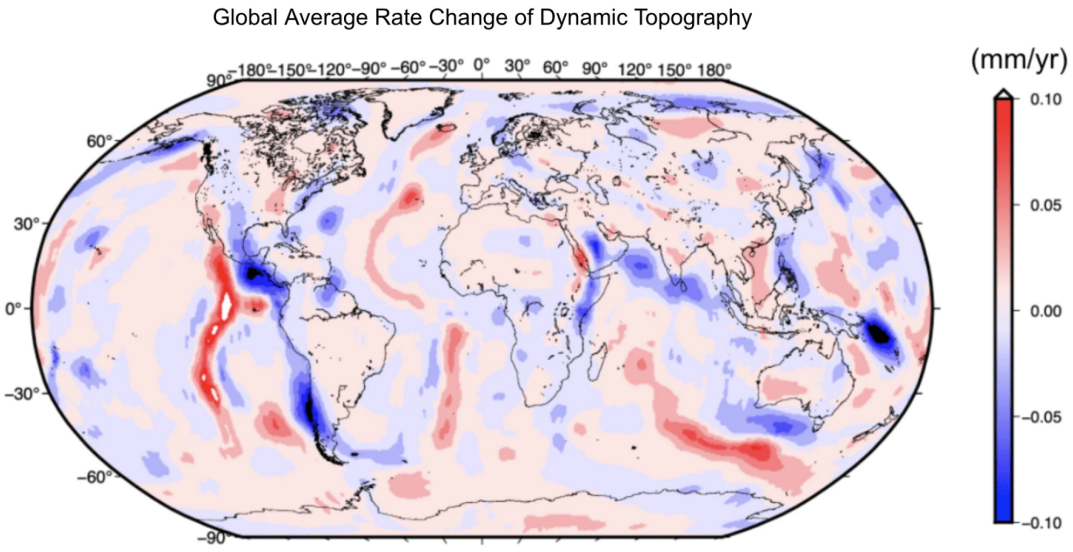

Figure 11. Rate change of global dynamic topographhty

The model in Figure 11 ranges from -0.143 mm/yr to 0.139 mm/yr. Though contributions are minor, the North American Atlantic Coast appears to be experiencing negitive dynamic topography. Figure 12 magnifies the variations of rates along the North American Atlantic Coast based on our final rate of change of DT solution.

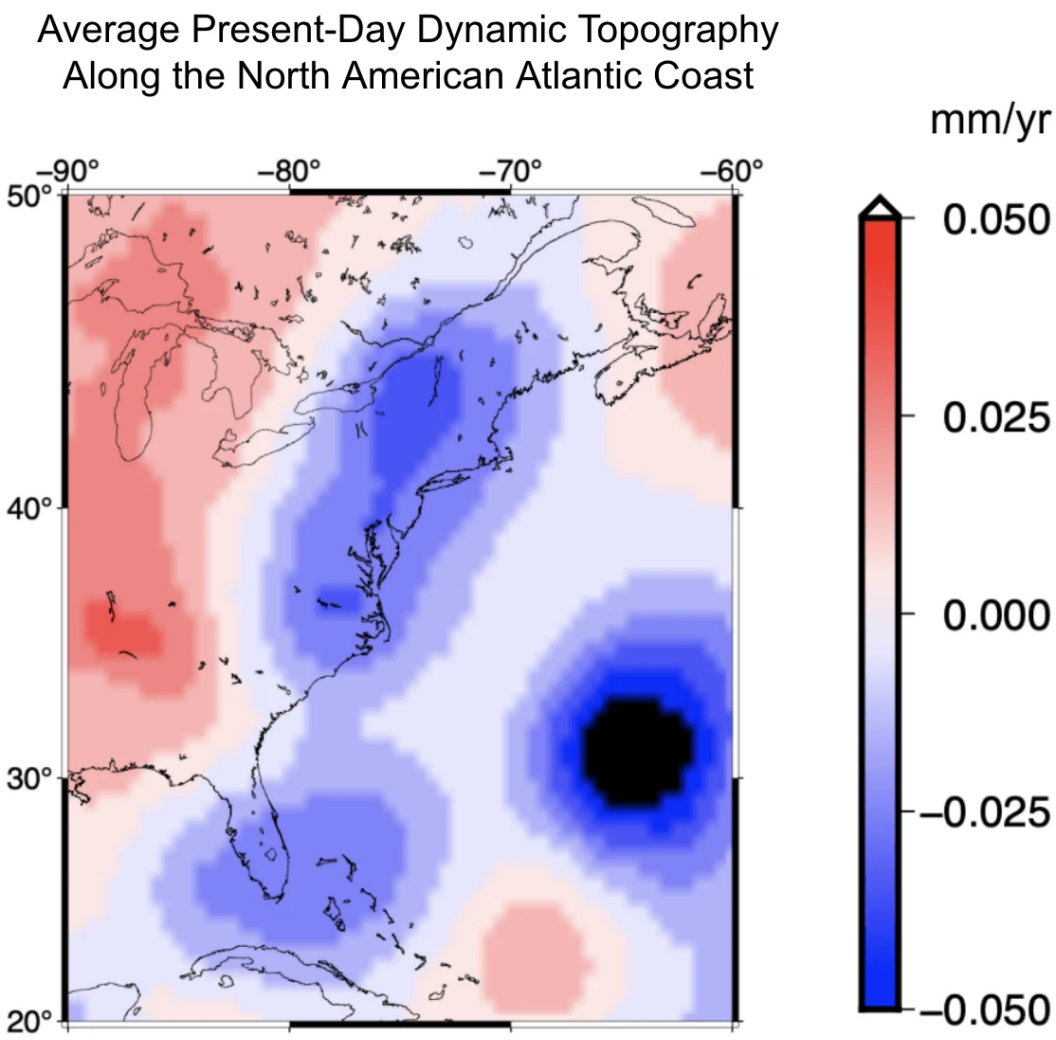

Figure 12. Rate change of dynamic topography along the North American Atlantic Coast

5. DISCUSSION

We analyze the differences in our instantaneous and rate change of DT models by plotting the residuals, calculated by subtracting our DT output from Austermann's output. Figure 12 shows the resulting residual for of the TX2008 Earth model with viscosity profile V1 and a no-slip BC imposed for instantaneous DT and average instantaneous DT.

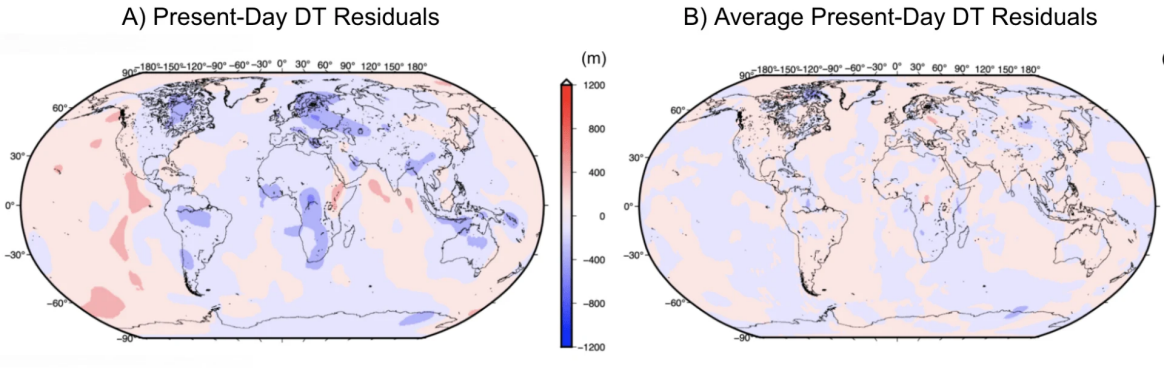

Figure 13. Residuals of the TX2008 Earth model with viscosity profile V1 and a no-slip BC imposed for instantaneous DT (left) and average instantaneous DT (right)

All six of our TX2008 Earth model setups compared favorably spatially, but showed wide variations in magnitude. Negative DT in our models with a no-slip BC applied and positive DT with the GPlates BC applied produced the largest residuals for instantaneous DT. Figure 13 shows the residuals for he TX2008 Earth model average with viscosity profile V1 and a no-slip BC imposed for rate change of DT and average rate change of DT.

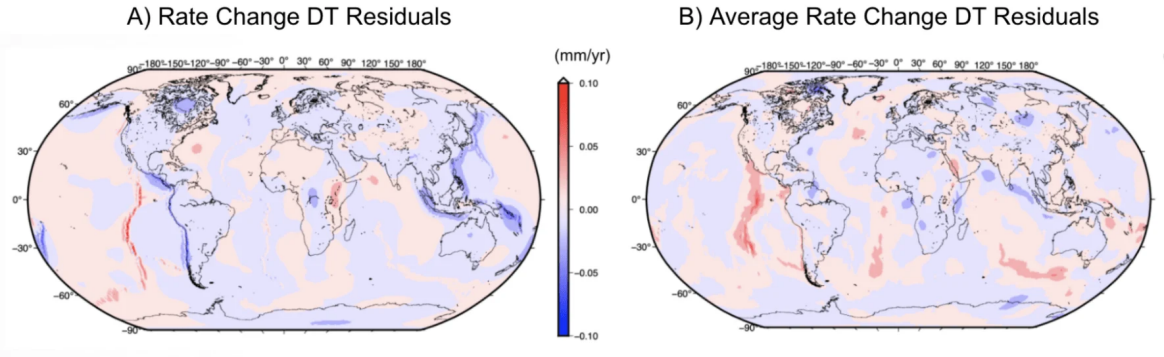

Figure 14. Residuals of the TX2008 Earth model average with viscosity profile V1 and a no-slip BC imposed for rate change of DT (left) and average rate change of DT (right).

The range for averge instantaneous DT residuals is -1162 m to 1605 m and the range for average rate change is -.048 mm/yr to .069 mm/yr. These large residuals may be misleading because they exist only in a few prominent features of the models.

Magnitude variations in temperature are likely contributing to the residuals observed, but should not account for this extent of variability. This indicates that the CBF algorithm may signifcantly influence the dynamic topography calculation; however, further analysis is required before confirming these residuals are a direct result of the CBF algorithm implementation.

Despite minor discrepencies, our results indicate that the North American Atlantic Coast is experiencing negative dynamic topography at a rate below 0.5 mm/yr, with some variability in magnitude along the coast. It is possible that specic regions are experiencing subsidence at a faster rate due to the influence of the Farallon slab. Our hypothesis was supported since the North American Atlantic region is experiencing subsidence with minor (<1 mm/yr) contributions from dynamic topography.

The main limitation of this study was that it did not include the S40RTS and SAVANI Earth models. However, these challenges of replicating the S40RTS and SAVANI setups exposed many of the issues with reproducibilty in ASPECT. As a result, we hope to start a discussion and work with the CIG community to move towards resolving some of these issues for other mantle convection researchers.

6. SUMMARY & NEXT STEPS

SUMMARY

Dynamic topography is thought to contribute to negative VLM along the North American Atlantic Coast. Local regions may be experiencing accelerated subsidence as a result of the fast velocity structures from the fragmented Farallon slab, which drives mantle downwelling. One objective of this study was to produce realistic estimates of the contribution of dynamic topography to negative VLM in the North American Atlantic Coast.

We model dynamic topography using the finite element code ASPECT (v2.2) to reproduce global rate change of dynamic topography following the methods of Austermann et al, (2017). Our purpose for replicating the Austermann study was to test the influence of the consistent boundary flux (CBF) algorithm for determining radial stresses at the boundaries. We compared model parameters, present-day DT models, and rate change of DT with Austermann et al, (2017) by evaluating structures in the model spatially and in magnitude. We produced our final rate change of DT solution by averaging rate change of DT for the 6 TX2008 Earth model setups we tested.

Because our model properties aligned well with the property solutions from Austermann et al, (2017), we suspect the implementation of the CBF algorithm significantly influences the dynamic topography calculation; however this will require further investigating. Our final results indicate that rate change of dynamic topgraphy is making slight (<0.5 mm/yr) contributions to subsidence in the North American Atlantic Coast.

NEXT STEPS

We will continue this project, focused on resolving issues that arose with the S40RTS and SAVANI Earth models. We will also investigate other factors that may be contributing to the large residuals we found in this study to better constrain the influence of the CBF algorithm.

Further, we are currently in the process of implementing a nonlinear rheology into our dynamic topography calculations. We expect this approach will produce more realistic estimates of dynamic topography and better constrain the contribution to VLM along the North American Atlantic Coast. We will compare those estimates to the final results we will generate from this study to assess the influence of a linear verus nonlinear rheology on dynamic topography.

ABSTRACT

Dynamic topography, defined as the deflection of the Earth's surface due to the convecting mantle, causes changes in vertical land motions (VLM). We aim to estimate the effect of dynamic topography on VLM along the North American Atlantic Coast, which is a region where land subsidence influences relative sea-level rise and other coastal hazards. The contribution of dynamic topography to VLM continues to be debated since previous studies show a range in the rate change of dynamic topography for this region, which are in part due to uncertainties in Earth's rheology. In this investigation, we model global mantle convection to better assess the role of dynamic topography on VLM along the North American Atlantic Coast. We are implementing a time-dependent approach using the finite element code ASPECT (v2.2.0). We constrain our initial temperature conditions using the tomography models SAVANI, GYPSUM, S40RTS, and TX2008 and then explore both linear and non-linear rheological models. The two rheological models allow us to assess differences in the rate change of dynamic topography globally with a nonlinear rheology compared to a linear rheology. We expect this work will allow us to better understand the contribution of dynamic topography to VLM along the North American Atlantic Coast.

REFERENCES

Auer, L., Boschi, L., Becker, T. W., Nissen-Meyer, T., & Giardini, D. (2014). Savani: A variable resolution whole-mantle model of anisotropic shear velocity variations based on multiple data sets. *Journal of Geophysical Research: Solid Earth*, *119*(4), 3006-3034.

Austermann, J., Mitrovica, J. X., Huybers, P., & Rovere, A. (2017). Detection of a dynamic topography signal in last interglacial sea-level records. *Science Advances*, *3*(7), e1700457.

Bertelloni, C. L., & Gurnis, M. (1997). Cenozoic subsidence and uplift of continents from time-varying dynamic topography. *Geology*, *25*(8), 735-738.

Braun, J. (2010). The many surface expressions of mantle dynamics. *Nature Geoscience*, *3*(12), 825-833.

Conrad, C. P., & Husson, L. (2009). Influence of dynamic topography on sea level and its rate of change. *Lithosphere*, *1*(2), 110-120.

Glišović, P., Forte, A. M., & Ammann, M. W. (2015). Variations in grain size and viscosity based on vacancy diffusion in minerals, seismic tomography, and geodynamically inferred mantle rheology. *Geophysical Research Letters*, *42*(15), 6278-6286.

Gurnis, M., Turner, M., Zahirovic, S., DiCaprio, L., Spasojevic, S., Müller, R. D., ... & Bower, D. J. (2012). Plate tectonic reconstructions with continuously closing plates. *Computers & Geosciences*, *38*(1), 35-42.

Hammond, W. C., Blewitt, G., Kreemer, C., & Nerem, R. S. (2021). GPS Imaging of Global Vertical Land Motion for Studies of Sea Level Rise. *Journal of Geophysical Research: Solid Earth*, *126*(7), e2021JB022355.

Karner, G. D. (1986). Effects of lithospheric in-plane stress on sedimentary basin stratigraphy. *Tectonics*, *5*(4), 573-588.

Liu, L. (2015). The ups and downs of North America: Evaluating the role of mantle dynamic topography since the Mesozoic. *Reviews of Geophysics*, *53*(3), 1022-1049.

Liu, S., & King, S. D. (2019). A benchmark study of incompressible Stokes flow in a 3-D spherical shell using ASPECT. *Geophysical Journal International*, *217*(1), 650-667.

Liu, L., Spasojević, S., & Gurnis, M. (2008). Reconstructing Farallon plate subduction beneath North America back to the Late Cretaceous. *Science*, *322*(5903), 934-938.

Lu, C., Grand, S. P., Lai, H., & Garnero, E. J. (2019). TX2019slab: A new P and S tomography model incorporating subducting slabs. *Journal of Geophysical Research: Solid Earth*, *124*(11), 11549-11567.

Molnar, P., England, P. C., & Jones, C. H. (2015). Mantle dynamics, isostasy, and the support of high terrain. *Journal of Geophysical Research: Solid Earth*, *120*(3), 1932-1957.

Ricard, Y., Richards, M., Lithgow-Bertelloni, C., & Le Stunff, Y. (1993). A geodynamic model of mantle density heterogeneity. *Journal of Geophysical Research: Solid Earth*, *98*(B12), 21895-21909.

Ritsema, J., Deuss, A. A., Van Heijst, H. J., & Woodhouse, J. H. (2011). S40RTS: a degree-40 shear-velocity model for the mantle from new Rayleigh wave dispersion, teleseismic traveltime and normal-mode splitting function measurements. *Geophysical Journal International*, *184*(3), 1223-1236.

Rowley, D. B., Forte, A. M., Moucha, R., Mitrovica, J. X., Simmons, N. A., & Grand, S. P. (2013). Dynamic topography change of the eastern United States since 3 million years ago. *science*, *340*(6140), 1560-1563.

Rubey, M., Brune, S., Heine, C., Davies, D. R., Williams, S. E., & Müller, R. D. (2017). Global patterns in Earth's dynamic topography since the Jurassic: the role of subducted slabs. *Solid Earth*, *8*(5), 899-919.

Schmid, C., Goes, S., Van der Lee, S., & Giardini, D. (2002). Fate of the Cenozoic Farallon slab from a comparison of kinematic thermal modeling with tomographic images. *Earth and Planetary Science Letters*, *204*(1-2), 17-32.

Simmons, N. A., Forte, A. M., & Grand, S. P. (2009). Joint seismic, geodynamic and mineral physical constraints on three-dimensional mantle heterogeneity: Implications for the relative importance of thermal versus compositional heterogeneity. *Geophysical Journal International*, *177*(3), 1284-1304.

Steinberger, B. (2007). Effects of latent heat release at phase boundaries on flow in the Earth's mantle, phase boundary topography and dynamic topography at the Earth's surface. *Physics of the Earth and Planetary Interiors*, *164*(1-2), 2-20.

Turcotte, D. L., & Schubert, G. (2002). *Geodynamics*. Cambridge university press.

Wolfgang Bangerth, Juliane Dannberg, Rene Gassmoeller, and Timo Heister. 2020. ASPECT v2.2.0. (version v2.2.0). Zenodo. https://doi.org/10.5281/ZENODO.3924604.

Yang, T., & Gurnis, M. (2016). Dynamic topography, gravity and the role of lateral viscosity variations from inversion of global mantle flow. *Geophysical Supplements to the Monthly Notices of the Royal Astronomical Society*, *207*(2), 1186-1202.

Zoback, M. L. (1992). First-and second-order patterns of stress in the lithosphere: The World Stress Map Project. *Journal of Geophysical Research: Solid Earth*, *97*(B8), 11703-11728.